

Is the glassy dynamics same in 2D as in 3D? The Adam Gibbs relation test

Santu Nath¹ and Shiladitya Sengupta^{1, a)}

Dept. of Physics, IIT Roorkee 47667 Uttarakhand, India.

It has been recognized of late that even amorphous, glass-forming materials in two dimensions (2D) are significantly affected by Mermin-Wagner type long wavelength thermal fluctuation which is inconsequential in three (3D) and higher dimensions. Thus any study of glassy dynamics in 2D should first remove the effect of such fluctuations. The present work considers the question of whether the role of spatial dimension on glassy dynamics is only limited to such fluctuations, or whether the nature of glassy dynamics is intrinsically different in 2D. We address this issue by studying the relationship between dynamics and thermodynamics within the framework of the Adam-Gibbs (AG) relation and its generalization the Random First Order Transition (RFOT) theory. Using two model glass-forming liquids we find that even after removing the effect of long wavelength fluctuations, the AG relation breaks down in two dimensions. Then we consider the effect of anharmonicity of vibrational entropy - a second factor highlighted recently that can qualitatively change the nature of dynamics. We explicitly compute the configurational entropy both with and without the anharmonic correction. We show that the anharmonic correction reduces the extent of deviation from the AG relation, but even after taking into account its effects, the AG relation still breaks down in 2D. It is also more prominent if one considers diffusion coefficient rather than α -relaxation time. Overall, the impact of the anharmonicity of vibration is larger than the long wavelength fluctuation in determining the qualitative relation between timescales and entropy. The extent and nature of deviation from the AG relation crucially depends on the attractive *vs.* repulsive nature of the inter-particle interaction. Thus our results suggest that the glassy dynamics in 2D may be intrinsically different from that in 3D.

^{a)}Electronic mail: shiladityasg@ph.iitr.ac.in

I. INTRODUCTION

It is well-known that the nature of phase transition can be qualitatively different in two dimensions (2D) than in three dimensions (3D)¹. For example, the Mermin-Wagner theorem argues that in 2D, a periodic structure will be unstable against long wavelength thermal deviation from equilibrium positions of atoms²⁻⁴. It raised doubt whether *crystalline* solids can exist in 2D. Later the KTHNY theory⁵⁻⁹ proposed a mechanism for liquid-to-crystal transition on a two dimensional elastic sheet that does not violate the Mermin-Wagner theorem. In this scenario, the translational and the rotational symmetries are broken at different temperatures. To the contrary, in 3D, they are both broken at the same temperature.

Liquids however can also transform into viscous supercooled liquids and eventually into *amorphous* solids, namely glass, by avoiding crystallization. Recently Flenner and Szamel¹⁰ have found that several hallmark features of glassy dynamics in 3D are different in 2D. The plateaus in the mean squared displacement (MSD) and in the two point density correlation functions are absent for large enough system sizes in 2D; qualitative and quantitative differences in the growth of dynamical heterogeneity and associated correlation length are also observed. These observations generated a lot of interest to understand the origin of these apparent differences. Shiba *et al.*¹¹ pointed out that in 2D, even *amorphous* matter should exhibit significant long wavelength thermal fluctuations, elucidated in the Mermin-Wagner theorem. It was shown that the effect of these fluctuations can be corrected for by considering the so-called cage-relative coordinates^{11,12} in which displacement of a particle is measured with respect to its nearest neighbours instead of from a fixed origin. Both computer simulation¹¹ as well as experimental studies in colloidal systems^{9,13} show that after introducing such corrections, dynamical quantities such as the MSD and the time correlation functions behave in qualitatively similar way in both two and three dimensions. These works highlight the role of long wavelength fluctuation as a new type of thermal fluctuation unique to 2D¹ and emphasize that this effect should be removed first before studying the glassy dynamics in 2D.

These results provide new insights about the dimension dependence of dynamics in glass-forming liquids. However they also raise fundamental questions that beg clarification. Since these previous studies focused on the *empirical description* of glassy dynamics, one wonders

whether the role of spatial dimension is fully explained by the long wavelength fluctuations, or whether the two dimensional glass-formers are intrinsically different from the three dimensional ones. This question is particularly significant for entropy-based glass transition theories, namely the Adam Gibbs (AG) relation¹⁴⁻¹⁶ and its generalization, the Random First Order Transition (RFOT) theory¹⁷⁻²². In these theories one first writes an expression for the free energy barrier for structural relaxation which depends on entropy, and thence estimates the structural relaxation time. The AG relation between the structural relaxation time τ_α and the configurational entropy S_c at a given temperature T is given by,

$$\tau_\alpha = \tau_\infty \exp\left(\frac{A}{TS_c}\right), \quad (1)$$

where A is an activation free energy barrier and τ_∞ is the limiting high temperature value of relaxation time. Eqn. 1 was originally introduced for polymer glass models in 3D, and the spatial dimension dependence is not explicit. To the contrary, the RFOT theory introduces a characteristic spatial correlation lengthscale ξ , so an explicit dimension dependence is plausible. However, in the RFOT framework, the lengthscale ξ is related to timescale and configuration entropy by a set of exponents which are *a priori unknown*. So an explicit dimension dependence is not guaranteed. In particular, whether the AG relation (Eqn. 1) is recovered as a special case of the RFOT relations, depends on the exponent values. Previously some of us found that the AG relation breaks down in 2D, while it remains valid in three and higher spatial dimensions²³. Given the recent discovery of the importance of Mermin-Wagner type excitations in 2D, the question naturally arises whether the observed deviation is a consequence of such low frequency vibrations, or whether spatial dimension has an intrinsic effect on the glass transition.

The long wavelength fluctuation affects dynamics (relaxation time), but not thermodynamics (configurational entropy), by definition. Within the potential energy landscape (PEL) formalism, the configurational entropy is usually computed by neglecting the anharmonic contribution to vibrational entropy²⁴⁻²⁶, see Sec. II for details. However, recently it has been observed that the anharmonic contribution is significant in the type of glass-formers we study here, and may even change the qualitative behaviour of a system²⁶.

Thus the goal of the present study is to critically examine the validity of the AG relation in 2D, after explicitly taking into account the effects of (i) Mermin-Wagner type fluctuations that affect dynamics and (ii) the anharmonic nature of vibration entropy that affect

thermodynamics. The rest of the paper is divided into the following sections: Sec. II defines the relevant quantities. Model glass-formers and simulation details are described in Sec. III. Sec. IV discusses the results of our analysis. Finally in Sec.V we summarize the results and conclude.

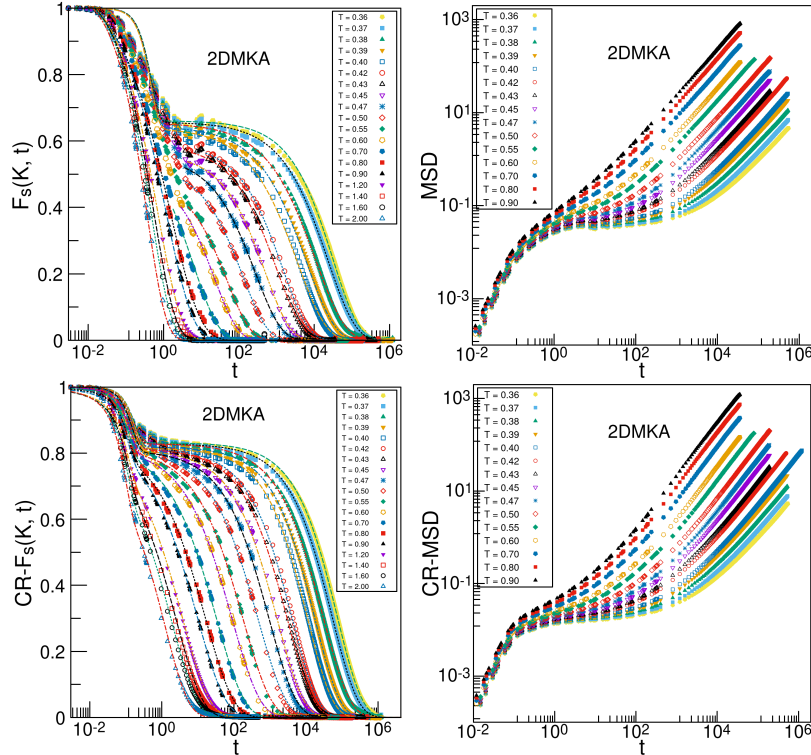


FIG. 1. Temperature dependence of the $F_s(K, t)$, MSD (top row) and $CR-F_s(K, t)$, CR-MSD (bottom row) for the 2DMKA model. Lines are fits to Eqn. 4.

II. DEFINITIONS

A. Dynamics

a. Cage relative (CR) displacement To correct for the long wavelength fluctuation in two dimensions, we compute the cage relative (CR) displacement of a particle i in a time interval $t^{11,12}$:

$$\Delta\vec{r}_{i,CR}(t) = \Delta\vec{r}_i(t) - \frac{1}{N_{nn}(i)} \sum_j \Delta\vec{r}_j(t), \quad (2)$$

where $N_{nn}(i)$ is the number of nearest neighbours of i , at $t = 0$, forming a transient cage around it. The right hand side of Eqn. 2, contains two terms. The first term $\Delta\vec{r}_i(t) =$

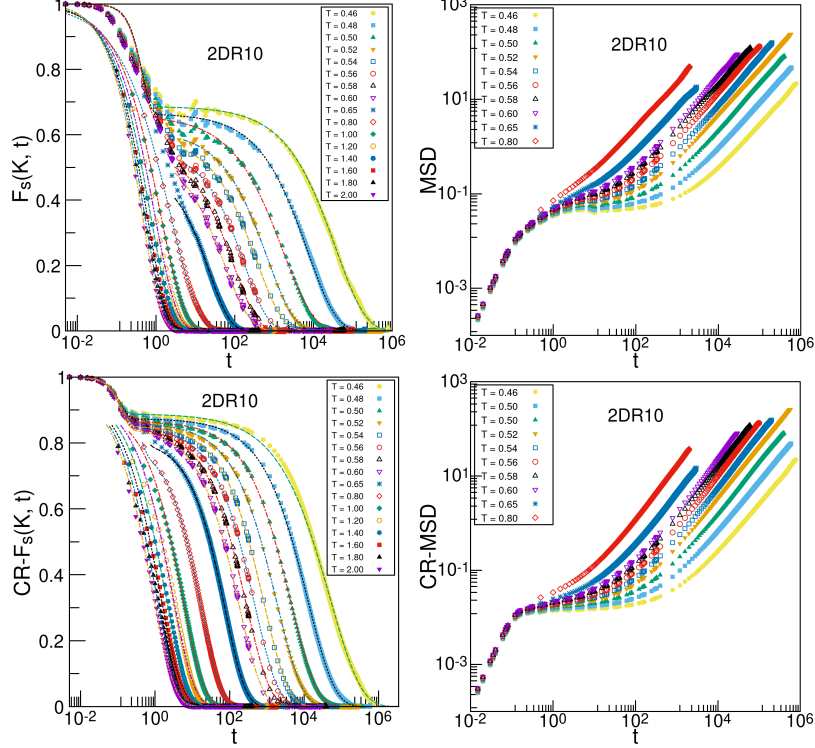


FIG. 2. Temperature dependence of the $F_s(K, t)$, MSD (top row) and the CR- $F_s(K, t)$, CR-MSD (bottom row) for the 2DR10 model. Lines are fits to Eqn. 4.

$\vec{r}_i(t + t_0) - \vec{r}_i(t_0)$ describes the actual displacement of the i -th particle in time interval t , with respect to a time origin t_0 . The second term represents the displacement of the center of mass of the nearest neighbours of particle i at time $t = 0$. Thus Eqn. 2 measures the displacement of the particle i relative to the center of mass of its nearest neighbours at $t = 0$.

b. Time correlation functions We analyze the dynamics using two point time correlation functions of instantaneous local density $\rho(\vec{r}, t) = \sum_{i=1}^N \delta(\vec{r} - \vec{r}_i(t))$ of N point particles. The standard self intermediate scattering function $F_s(\vec{K}, \tau)$ is defined as,

$$\begin{aligned}
 F_s(\vec{K}, \tau) &= \frac{1}{N} \langle \rho(\vec{K}, t_0 + \tau) \rho(-\vec{K}, t_0) \rangle \\
 &= \frac{1}{N} \sum_{i=1}^N \langle e^{-i\vec{K} \cdot [\vec{r}_i(t_0 + \tau) - \vec{r}_i(t_0)]} \rangle \\
 &= \frac{1}{N} \sum_{i=1}^N \langle e^{-i\vec{K} \cdot \vec{r}_i(t_0 + \tau)} \times e^{i\vec{K} \cdot \vec{r}_i(t_0)} \rangle
 \end{aligned} \tag{3}$$

where $\rho(\vec{K}, t) = \int d\vec{r} \rho(\vec{r}, t) e^{-i\vec{K} \cdot \vec{r}} = \sum_{i=1}^N e^{-i\vec{K} \cdot \vec{r}_i(t)}$ is the Fourier transform of $\rho(\vec{r}, t)$. $\langle \cdot \rangle \equiv \frac{1}{N_{t_0}} \sum_{t_0=1}^{N_{t_0}} \cdot$ represents averaging over different time origins t_0 . Since the liquid is isotropic,

the correlation function depends only on the magnitude of the wave vector \vec{K} . Thus we further do a averaging over different directions, to compute a correlation function $F_s(K, \tau)$ that depends only on the magnitude $K = |\vec{K}|$. We chose K at the first peak of the static structure factor $S(K)$.

In addition, we report data obtained from another time correlation function - the overlap function. The details are described elsewhere²³.

We define cage-relative self-intermediate scattering function (CR- $F_s(K, t)$) as the time correlation function using the cage relative displacement replacing standard displacement in Eqn. 3.

c. α -relaxation time (τ_α) From time correlation functions $F_s(K, t)$ and CR- $F_s(K, t)$, the structural relaxation time τ_α characterizing the dynamics of standard and cage-relative displacement fields is estimated by fitting $y(t)$ to the following functional form:

$$y(t) = (1 - f_c) e^{-(t/\tau_s)^2} + f_c e^{-(t/\tau_\alpha)^\beta} \quad (4)$$

where $y(t)$ denotes the appropriate time correlation function. The first term describes the short time decay and the second term the long time α decay of the correlation function. f_c, τ_s and β denote the plateau height, the characteristic time scale for short time decay and the Kohlrausch-Williams-Watts exponent respectively. In addition, we also estimate τ_α from the overlap function of standard displacement field the details of which is described in Ref.²³.

d. Mean Squared displacement Standard mean squared displacement (MSD) and its cage-relative generalization CR-MSD are defined as

$$\begin{aligned} \text{MSD}(t) &= \left\langle \frac{1}{N} \sum_{i=1}^N [\Delta \vec{r}_i(t)]^2 \right\rangle \\ \text{CR-MSD}(t) &= \left\langle \frac{1}{N} \sum_{i=1}^N [\Delta \vec{r}_{i,CR}(t)]^2 \right\rangle \end{aligned} \quad (5)$$

where $\Delta \vec{r}_i(t), \Delta \vec{r}_{i,CR}(t)$ are defined in Eqn. 2. $\langle \cdot \rangle$ denotes the ensemble average.

e. Diffusion coefficient We estimate the diffusion coefficient from the MSD and CR-MSD using the definition

$$\begin{aligned} D &= \lim_{t \rightarrow \infty} \frac{\text{MSD}(t)}{4t} \\ D_{CR} &= \lim_{t \rightarrow \infty} \frac{\text{CR-MSD}(t)}{4t} \end{aligned} \quad (6)$$

B. Thermodynamics

1. Configurational entropy S_c in harmonic approximation

Within the potential energy landscape formalism²⁴, the configurational entropy $S_c(T)$ is a measure of the number of independent potential energy minima that a system can sample at a given temperature T and a given density ρ . It is defined as the ensemble-averaged difference between the total and the vibrational entropy:

$$\begin{aligned} S_c &\equiv S_{total}(T) - S_{vib}(T) \\ S_c^{har}(T) &= S_{total}(T) - S_{vib}^{har}(T). \end{aligned} \quad (7)$$

where S_{vib}^{har} indicates that the vibrational entropy is computed using the the harmonic approximation^{25,27}.

The total entropy of the liquid S_{total} at a given temperature and density is computed using thermodynamic integration method, the details of which is described elsewhere^{25,27}.

2. (Vibrational) potential energy (PE)

a. Harmonic approximation At a given temperature T , the average per-particle (vibrational) potential energy in the harmonic approximation in 2D can be written as (setting the Boltzmann constant $k_B = 1$),

$$U_{har}(T) = \langle U_{IS}(T) \rangle + \frac{2}{2}T \quad (8)$$

Here $\langle U_{IS} \rangle$ is the per particle potential energy at a minimum (inherent structure, IS). We explicitly show the $\langle \cdot \rangle$ to emphasize that it is ensemble averaged.

b. Anharmonic correction The average anharmonic contribution $U_{anhar}(T)$ to the (vibrational) per-particle potential energy can be found by subtracting the harmonic component of potential energy from the full potential energy²⁴⁻²⁶, *i.e.*

$$U_{anhar} \equiv U - U_{har} \quad (9)$$

We have computed $U_{anhar}(T)$, using two methods differing in the averaging procedure, leading to two slightly different estimates of S_c . The methods are described below.

3. Anharmonic vibrational entropy: method 1

a. Anharmonic correction to (vibrational) PE $U_{anhar}(T)$ is computed using the following procedure:

$$\begin{aligned} U_{anhar}(T) &= \langle U(T) \rangle - \langle U_{IS}(T) \rangle - \frac{2}{2}T \\ &= \sum_{j=2}^{j_{max}} C_j T^j \end{aligned} \quad (10)$$

where we used Eqn. 8. Here $\langle U(T) \rangle$ is the average potential energy per particle at a temperature T . The second line describes the temperature dependence of U_{anhar} by a fit polynomial with C_j 's being the unknown fit parameters²⁴.

b. Anharmonic vibrational entropy From Eqn. 10, the anharmonic component of vibrational entropy can be written as,

$$S_{vib}^{anhar}(T) = \int_0^T dT' \frac{1}{T'} \frac{\partial U_{anhar}(T')}{\partial T'} = \sum_{j=2}^{j_{max}} \frac{j}{j-1} C_j T^{j-1} \quad (11)$$

4. Anharmonic vibrational entropy: method 2

a. Anharmonic correction to (vibrational) PE In this method the (vibrational) potential energy in a given basin at a given temperature T is directly estimated. Starting from inherent structures obtained by minimizing configurations equilibrated at a parent temperature T_p , short molecular dynamics (MD) runs of duration \approx MSD plateau time are performed at different target temperatures $T \leq T_p$. The anharmonic contribution is then

computed from

$$\begin{aligned}
U_{anhar}(T, T_p) &= \langle U(T) - U_{IS}(T_p) \rangle - \frac{2}{2}T \\
&= \sum_{j=2}^{j_{max}} C_j(T_p) T^j
\end{aligned} \tag{12}$$

Here $C_j(T_p)$'s are T_p dependent unknown fit parameters.

b. Anharmonic vibrational entropy In method 2, the anharmonic contribution to vibrational entropy is computed from Eqn. 12 as,

$$\begin{aligned}
S_{vib}^{anhar}(T_p) &= \int_0^{T_p} dT' \frac{1}{T'} \frac{\partial U_{anhar}(T', T_p)}{\partial T'} \\
&= \sum_{j=2}^{j_{max}} \frac{j}{j-1} C_j(T_p) T_p^{j-1}
\end{aligned} \tag{13}$$

5. Anharmonic configurational entropy

Finally, the configurational entropy with the anharmonic correction to vibrational entropy is given by,

$$S_c^{anhar}(T) = S_{total}(T) - \left(S_{vib}^{har}(T) + S_{vib}^{anhar}(T) \right) \tag{14}$$

TABLE I. Parameters for fit to the high temperature Arrhenius relation: $\tau_\alpha(T) = \tau_\infty \exp(E_0/k_B T)$ and the low temperature VFT formula: $\tau_\alpha(T) = \tau_0 \exp(\frac{D}{T-T_0})$ for 2DMKA and 2DR10 models.

| Model | Correlation function | Fit function | Temperature range | τ_∞ | E_0 | τ_0 | D | T_0 |
|-------|----------------------|--------------|-------------------|---------------|-------|----------|------|-------|
| 2DMKA | CR- $F_s(K, t)$ | Arrhenius | 0.80 - 2.00 | 0.24 | 3.26 | - | - | - |
| | CR- $F_s(K, t)$ | VFT | 0.36 - 0.80 | - | - | 0.42 | 2.27 | 0.18 |
| | overlap function | VFT | 0.36 - 0.80 | - | - | 0.12 | 2.11 | 0.19 |
| | $F_s(K, t)$ | VFT | 0.36 - 0.80 | - | - | 0.05 | 2.66 | 0.16 |
| 2DR10 | CR- $F_s(K, t)$ | Arrhenius | 0.80 - 2.00 | 0.13 | 3.73 | - | - | - |
| | CR- $F_s(K, t)$ | VFT | 0.46 - 0.80 | - | - | 0.62 | 1.56 | 0.32 |
| | overlap function | VFT | 0.46 - 0.80 | - | - | 0.17 | 1.65 | 0.32 |
| | $F_s(K, t)$ | VFT | 0.46 - 0.80 | - | - | 0.03 | 2.32 | 0.29 |

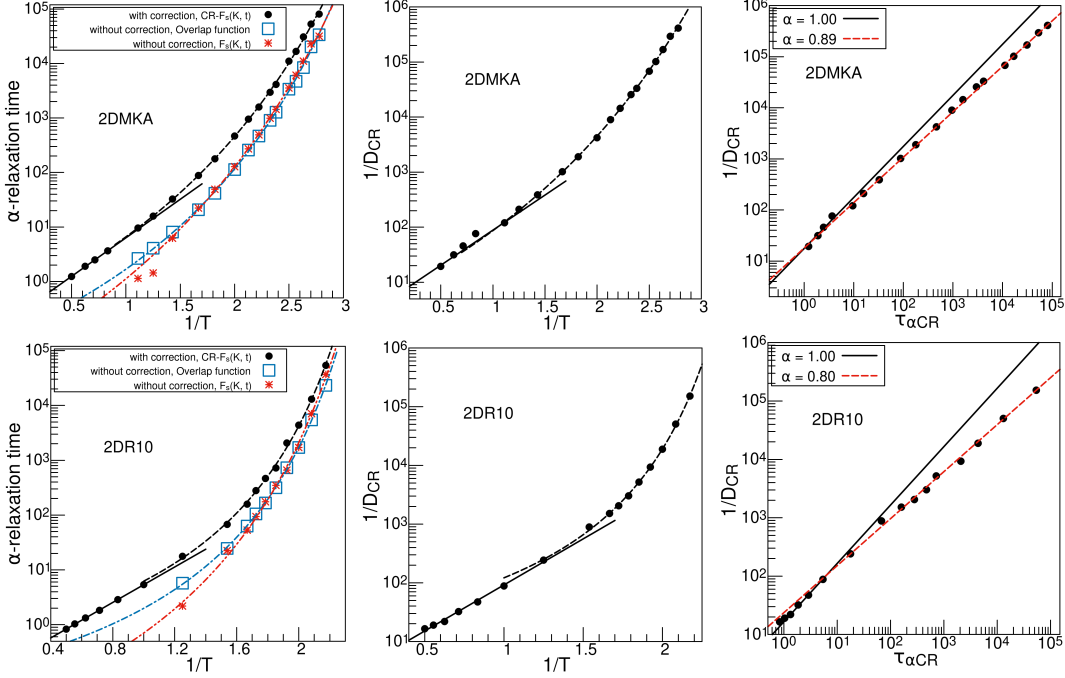


FIG. 3. *Effect of long wavelength fluctuations on characteristic timescales.* Inverse temperature dependence of characteristic timescales are shown for the 2DMKA (top row) and the 2DR10 (bottom row) respectively. Time scales are (a) τ_α computed from the standard intermediate scattering function as well as from the standard overlap function (reported in Ref.²³), (b) $\tau_{\alpha CR}$ estimated from the cage-relative intermediate scattering function, and (c) diffusion coefficient D_{CR} obtained from the cage-relative MSD. Data at low temperatures are fitted to the VFT equation: $\tau_\alpha = \tau_0 \exp\left(\frac{D}{T-T_0}\right)$, $D_{CR}^{-1} = (D_{CR}^{-1})_0 \exp\left(\frac{D}{T-T_0}\right)$ while the high T data are fitted to the Arrhenius equation $\tau_\alpha(T) = \tau_\infty \exp\left(\frac{E_0}{k_B T}\right)$. Fit parameters are listed in Table I. τ_α from the overlap function are scaled by a constant factor of 0.475 (2DMKA) and 0.043 (2DR10) to match with τ_α values from $F_s(K, t)$. *Stokes-Einstein Breakdown:* On the right most column, comparison of the diffusion time scale D_{CR} and the α -relaxation time scale $\tau_{\alpha, CR}$ from the cage-relative displacement show that they are coupled at high temperature, but gets decoupled at low temperatures, indicating breakdown of the Stokes Einstein relation. Taken together these data show that long wavelength fluctuation makes the α -relaxation time longer, but the qualitative behaviour of the dynamics is not affected.

III. MODELS AND SIMULATION DETAILS

NVT molecular dynamics simulations using the Brown and Clarke thermostat²⁸ were done for the following two dimensional glass-former models. The simulation details are the same as in Ref.²³.

A. 2D MKA model

The binary mixture ($A_{80}B_{20}$) of Lennard Jones particles introduced by Kob and Andersen (KA)²⁹ is a model glass forming liquid in three dimensions. In the case of the modified KA (MKA) model in two dimensions (2D), the composition is set to $A_{65}B_{35}$ ³⁰. The interaction potential, including correction terms that make both potential energy and force to go to zero smoothly at the cutoff, is given by:

$$V_{\alpha\beta}(r) = \begin{cases} 4\epsilon_{\alpha\beta} \left[\left(\frac{\sigma_{\alpha\beta}}{r}\right)^{12} - \left(\frac{\sigma_{\alpha\beta}}{r}\right)^6 \right] + 4\epsilon_{\alpha\beta} \left[c_0 + c_2 \left(\frac{r}{\sigma_{\alpha\beta}}\right)^2 \right], & r < \text{cutoff} \\ 0, & r > \text{cutoff} \end{cases}, \quad (15)$$

where $\alpha, \beta \in \{A, B\}$. Units of length, energy are σ_{AA} , ϵ_{AA} respectively. $\epsilon_{AB} = 1.5$, $\epsilon_{BB} = 0.5$, $\sigma_{AB} = 0.80$, $\sigma_{BB} = 0.88$. The cutoff is at $2.5\sigma_{\alpha\beta}$. Simulations were done at a fixed number density $\rho = 1.20\sigma_{AA}^{-3}$ with system size $N = 2000$ for a temperature range $\frac{k_B T}{\epsilon_{AA}} = 0.36 - 2.00$. The MD integration time step was in the range $dt/(\sqrt{\sigma_{AA}^2/\epsilon_{AA}}) = 0.003 - 0.005$, with smaller dt values used at higher temperatures. For this model the onset temperature is $T_{onset} = 0.80$. It serves as the reference temperature to differentiate between the low and the high T regimes. For $T > 0.90$ (reduced units), only single trajectory has been chosen and for $T < 0.90$, 4-5 independent trajectories were analyzed. The runlength for all trajectories analyzed is more than $100\tau_\alpha$.

B. 2D R10 model

It is a 50:50 binary mixture of purely repulsive soft disks in two dimensions³¹, with a inverse power law exponent 10. The interaction potential is given by,

$$V_{\alpha\beta}(r) = \begin{cases} \epsilon \left[\left(\frac{\sigma_{\alpha\beta}}{r} \right)^{10} \right] + \epsilon \left[c_0 + c_2 \left(\frac{r}{\sigma_{\alpha\beta}} \right)^2 + c_4 \left(\frac{r}{\sigma_{\alpha\beta}} \right)^4 \right], & r < \text{cutoff} \\ 0, & r > \text{cutoff} \end{cases} \quad (16)$$

where $\alpha, \beta \in \{A, B\}$. $\epsilon = 1.0$, $\sigma_{AA} = 1.0$ and $\sqrt{\frac{\sigma_{AA}^2}{\epsilon_{AA}}}$ set the units of energy, length and time respectively. $\sigma_{BB} = 1.40$, $\sigma_{AB} = 1.18 \neq \frac{\sigma_{AA} + \sigma_{BB}}{2}$, $c_0 = -0.806140903539923$, $c_2 = 0.7$, $c_4 = -0.156300219287607$ represent the correction to make the potential vanish at cutoff = $1.385418025 \sigma_{\alpha\beta}$ continuously upto the second derivative. Simulations were done at a number density of $\rho \sigma_{AA}^3 = 0.85$ over a range of temperatures $\frac{k_B T}{\epsilon_{AA}} = 0.46 - 2.00$, for a system size of $N = 2048$. The onset temperature is at $T_{onset} = 0.80$ (reduced units) which demarcates the high and low temperature regimes. For $\frac{k_B T}{\epsilon_{AA}} \geq 1.00$, a single trajectory has been chosen with integration time step $dt / (\sqrt{\sigma_{AA}^2 / \epsilon_{AA}}) = 0.003$ and for $T \leq T_{onset}$ 3-5 independent trajectories were used with $dt / (\sqrt{\sigma_{AA}^2 / \epsilon_{AA}}) = 0.005$. The runlength for all trajectories analyzed is more than $100 \tau_\alpha$.

C. Simulations for anharmonic correction by method 2

To compute the anharmonic correction by method 2 described in Sec. II, MD runs were performed for short time duration \sim MSD plateau time. These runs were started from inherent structures obtained from various parent temperatures T_p . The range of T_p values were chosen to be $T_p = 0.36 - 0.90$ for the 2DMKA model and $T_p = 0.46 - 0.80$ for the 2DR10 model respectively. Number of runs were 26-926 for the 2DMKA model and 1000-3985 for the 2DR10 model depending on the temperature. For the same initial configuration, runs were performed at various target temperatures T from 10^{-6} upto T_p . At all target temperatures T , runlengths were chosen to be for 1000 MD steps for the 2DMKA model and 3000 MD steps for the 2DR10 model. Integration time step was set to $dt / (\sqrt{\sigma_{AA}^2 / \epsilon_{AA}}) = 0.003$ for both models.

IV. RESULTS

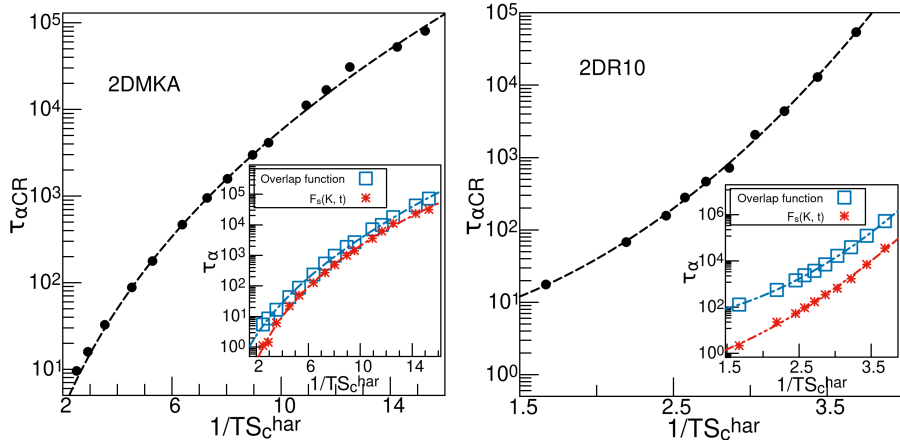


FIG. 4. *Effect of long wavelength fluctuations on the Adam-Gibbs (AG) relation. (Inset panels):* The AG plots without any correction, *i.e.* relaxation time τ_{α} is computed from correlation functions of standard displacement field and configuration entropy S_c^{har} computed within harmonic approximation. Data for S_c^{har} and τ_{α} from overlap function was taken from Ref.²³. In the present work, we have added the τ_{α} data obtained from $F_s(K, t)$. (*Main panels*): The AG plots with relaxation time ($\tau_{\alpha CR}$) corrected for the long wavelength fluctuations *vs.* $\frac{1}{TS_c^{har}}$. We show configuration entropy in harmonic approximation to compare with the reference data and isolate the effect of long wavelength fluctuations. Lines are fits to the generalized Adam-Gibbs's relation $\ln \tau_{\alpha} = \ln \tau_0 + A \left(\frac{1}{TS_c} \right)^{\alpha}$. See text for further details and Table III for fit parameter values.

A. Comparison of standard *vs.* cage-relative dynamics

In Figs. 1 and 2 we compare the dynamics for the 2DMKA and the 2DR10 models respectively using two estimators: the intermediate scattering functions and the MSD. The estimators computed from standard displacement field are shown in the top rows and those from the cage-relative coordinates are displayed in bottom rows. Both standard and cage-relative estimators show qualitative signatures of glassy dynamics³². However, we note the *quantitative* differences: (a) the plateau regime is more prominent for cage-relative $F_s(K, t)$ and MSD, (b) plateau height f_c of the cage-relative intermediate scattering function is higher and (c) the transient wiggle in the plateau regime of the cage-relative $F_s(K, t)$ due to

finite size effect is absent in both the models. These observations are in sync with previous studies¹¹.

Next we study the effect of long wavelength fluctuations on the slowdown of dynamics with reducing temperature. First we compute the usual τ_α from the dynamics of the standard displacement field in Fig. 3 left columns. Note that Ref.²³ used the overlap function while the present study analyzes the $F_s(K, t)$. We show for both the models that τ_α extracted from either correlation function are mutually proportional. More interestingly, we extract $\tau_{\alpha CR}$ from the cage-relative intermediate scattering function. We see that the main effect of the long wavelength fluctuation is quantitative: the cage-relative displacement field has longer α -relaxation timescale. This finding is consistent with previous observations⁹. However, the T dependence of the timescales are similar, as the VFT fit $\tau_\alpha(T) = \tau_0 \exp(\frac{D}{T-T_0})$ to τ_α from both the $F_s(K, t)$ and the CR- $F_s(K, t)$ yield similar divergence temperature T_0 and kinetic fragility $\frac{T_0}{D}$, see Table I. For the sake of completeness, we also show the high T Arrhenius fit to CR- $F_s(K, t)$ timescale to mark the onset temperature of non-Arrhenius dynamics.

In the low T non-Arrhenius regime, the various characteristic timescales such as the α -relaxation time and the diffusion coefficient becomes decoupled - a phenomenon usually labelled as the breakdown of the Stokes-Einstein relation (SEB). Consequently, in the context of testing the AG and the RFOT relations an interesting open question is the choice of timescale to characterize dynamics, which the theories does not explicitly specify. Some of us in a previous study³³ showed that for the AG relation, the diffusion coefficient is the more fundamental choice of timescale. Thus we also characterize dynamics by extracting the diffusion coefficient D_{CR} from the cage-relative MSD, see middle panels of Fig. 3. In the right columns of Fig. 3, we compare the time scales $\tau_{\alpha CR}$ and the D_{CR} and find a decoupling (SEB) at low temperatures. Thus taken together, these observations indicate that the long wavelength fluctuation affects the dynamics in 2D quantitatively, but qualitative features of the dynamics remains the same.

B. Effect of the long wavelength fluctuation on the AG relation

After accounting for the long wavelength fluctuation in dynamics, we pose the next natural question: how does the relation between dynamics and thermodynamics gets affected by such long wavelength fluctuations? To answer it, one is required to test the AG relation with-

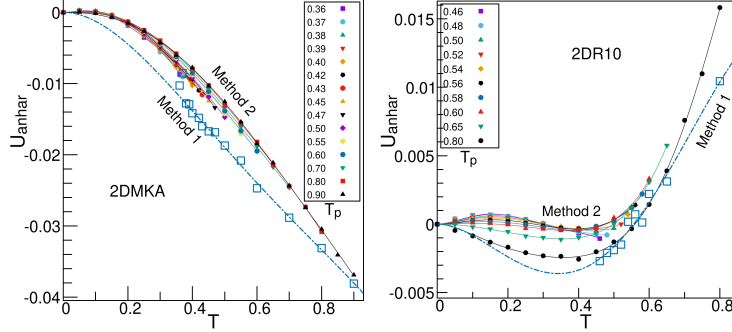


FIG. 5. Temperature dependence of anharmonic correction to vibrational potential energy $U_{anhar}(T)$ for the 2DMKA and the 2DR10 models respectively. $U_{anhar}(T)$ is computed using two different methods, see Sec II. For both models, lines are fits to fourth order polynomials ($j_{max} = 4$ in Eqns. 10 and 12).

out (standard) and with (cage-relative) correction due to the long-wavelength fluctuations. The AG relation predicts a linear dependence of $\ln \tau_\alpha$ on $(TS_c)^{-1}$ at all spatial dimension D , Eqn.1. According to the RFOT theory¹⁷⁻²², the growing many body correlation at lowering temperature is characterized by a growing static correlation length ξ . The free energy barrier for structural relaxation ΔG scales with ξ as $\Delta G \sim \xi^\psi$. Thus the characteristic time scale for structural relaxation scales with ξ as: $\tau_\alpha \sim \exp(\frac{\Delta G}{k_B T}) \sim \exp(\frac{\xi^\psi}{k_B T})$. Further, in the RFOT scenario, the correlation length is related to the configurational entropy as: $\xi^{D-\theta} \sim \frac{1}{S_c}$. Hence the relation between time and entropy becomes explicitly dimension dependent:

$$\tau_\alpha \sim \exp\left(\frac{A}{(TS_c)^{\frac{\psi}{D-\theta}}}\right) \quad (17)$$

The RFOT exponents ψ and θ are in general unknown. However, they should satisfy the inequality²¹: $\theta \leq \psi \leq D - 1$. Note that testing the RFOT relations require computation of the lengthscale ξ which is beyond the scope of the present study. However, guided by these scaling relations we fit the data to a non-linear, generalized AG form:

$$\ln \tau_\alpha = \ln \tau_0 + A\left(\frac{1}{TS_c}\right)^\alpha \quad (18)$$

The AG relation is recovered^{21,34} for $\psi = D/2 = \theta$.

Fig. 4 tests the relationship between the α -relaxation timescale and the configurational entropy for the 2DMKA and the 2DR10 models. In all cases the temperature range is chosen upto the onset temperature. Here the configurational entropy is computed using

the harmonic approximation, to isolate the effect of long wavelength fluctuation on the AG relation. The inset panels show the timescales τ_α without correcting for the long wavelength fluctuation, obtained from both the overlap function (Ref²³) as well as the $F_s(K, t)$. Comparing the timescales from the intermediate scattering function without (standard) and with (cage-relative) correction due to the long wavelength fluctuation, we see its main effect is *quantitative*: in both cases the AG relation still breaks down, and instead follows the non-linear form in Eqn. 18. However, removing the effects of long wavelength fluctuation changes the extent of the deviation from linearity, *i.e.* values of the exponent $\alpha \equiv \frac{\psi}{D-\theta}$, see Table III. Interestingly, for the 2DMKA model, α increases *towards* 1 whereas for the 2DR10 model, α increases *away* from 1. Thus the nature of deviation depends on the nature of the interatomic potential.

TABLE II. Parameters for fit to the temperature (T) dependence of TS_c for the 2DMKA and the 2DR10 models, Fig. 6. $\alpha_1 = 1$ represents linear fit $TS_c = [K_T(\frac{T}{T_K}) - 1]$ and $\alpha_1 \neq 1$ sets depict non-linear fit to $TS_c = [K_T(\frac{T}{T_K}) - 1]^{\frac{1}{\alpha_1}}$. Anharmonic 1 and 2 refer to anharmonic correction to S_c computed by methods 1 and 2 respectively.

| Model | S_c type | K_T | T_K | α_1 |
|-------|--------------|-------|-------|------------|
| 2DMKA | Harmonic | 0.16 | 0.25 | 1 |
| | Harmonic | 0.16 | 0.28 | 1.10 |
| | Anharmonic 1 | 0.26 | 0.10 | 0.68 |
| | Anharmonic 2 | 0.26 | 0.11 | 0.67 |
| 2DR10 | Harmonic | 0.17 | 0.18 | 1 |
| | Harmonic | 0.19 | 0.20 | 1.05 |
| | Anharmonic 1 | 0.11 | 0.35 | 2.14 |
| | Anharmonic 2 | 0.05 | 0.05 | 0.60 |

C. Effect of anharmonic vibration on the AG relation

Details of configurational entropy calculation in harmonic approximation (Eqn. 7) for the 2DMKA and the 2DR10 models have been reported elsewhere²³. Here we describe the effect of adding anharmonic correction to S_c (Eqn. 14). First, in Fig. 5 we show the tem-

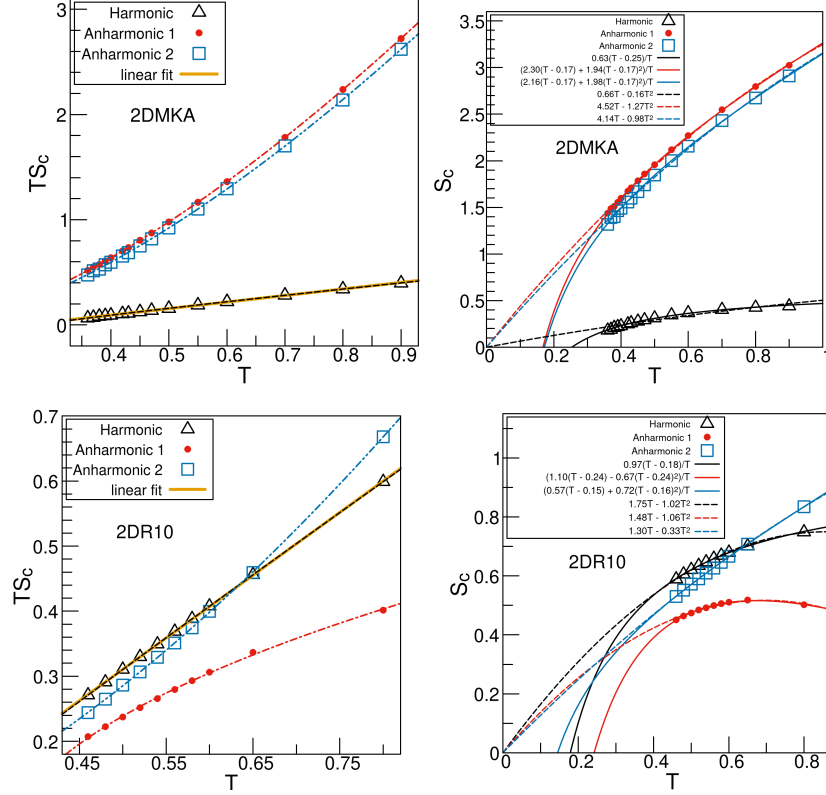


FIG. 6. *Effect of anharmonic vibration on the T dependence of configuration entropy. TS_c vs. Temperature (left column) for the 2DMKA (top row) and the 2DR10 (bottom row) models. S_c is computed in harmonic approximation (black circles, Eqn. 7) as well as by adding anharmonic correction (Eqn. 14) using two different methods (Eqns. 10 - 13). Linear fit ($\alpha = 1$) represent the function: $TS_c = [K_T(\frac{T}{T_K} - 1)]$. To check the deviation from linearity, we fit the data to a generalized non-linear temperature dependence: $TS_c = [K_T(\frac{T}{T_K} - 1)]^{\frac{1}{\alpha_1}}$ where T_K is the Kauzmann temperature, and K_T is the thermodynamic fragility, and α_1 is a free parameter. Parameter values are listed in Table II. Right column shows the T dependence of S_c without (black circle) and with anharmonic correction using methods 1 and 2. Fit lines test two types of plausible temperature dependence of S_c - one with $T_K = 0$ and the other with $T_K \neq 0$. Our data is consistent with either scenarios. See text for more details.*

perature dependence of the anharmonic contribution to the potential energy characterized by polynomial fit functions, see Sec II and Eqns. 9, 10 and 12.

Analysis within the PEL framework has shown that for harmonic approximation to the vibrational entropy, TS_c should be linear in T : $TS_c = [K_T(\frac{T}{T_K} - 1)]$, where $S_c(T_K) = 0$ determines the Kauzmann temperature T_K and K_T is the thermodynamic fragility^{35,36}. This

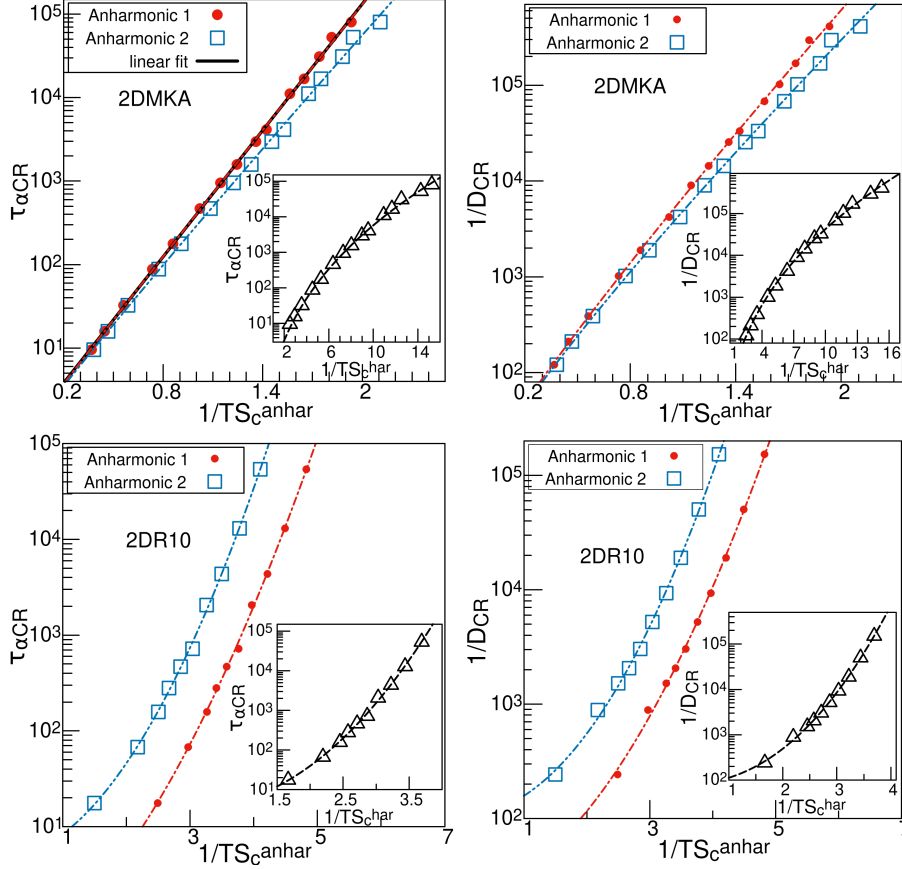


FIG. 7. *Effect of anharmonic correction to configurational entropy on the AG relation:* The AG plot in terms of both α -relaxation time $\tau_{\alpha CR}$ (left column) and diffusion coefficient D_{CR} for the 2DMKA (top row) and the 2DR10 models (bottom row). The inset shows configuration entropy in harmonic approximation, and the main panel describes S_c^{anhar} where anharmonic vibration effects are explicitly included. $\tau_{\alpha CR}$ is computed from the CR- $F_s(K, t)$. Linear fits represent the AG relation (see Eqn. 1). Non-linear curves are fits to the generalized Adam-Gibbs's relation $\ln \tau_{\alpha} = \ln \tau_0 + A(1/TS_c)^{\alpha}$, see Eqn. 18 and Table III for fit parameter values. For the 2DMKA model the AG relation is recovered after incorporating the anharmonic correction, but it still breaks down for the 2DR10 model even after correction due to long wavelength fluctuations and anharmonic vibration are implemented. Thus our data demonstrates intrinsic dimension dependence of the physics of glass transition. See text for further details.

expectation is well tested for 3D glass-former models in experiments³⁷, and also in simulation studies without³⁸ and with anharmonic corrections²⁵ although deviations have also been noted³⁹. Recently Berthier *et al.* has raised³⁹ the intriguing possibility that the Kauzmann

TABLE III. Table of the coefficient A , exponent α and τ_0 values in the generalized AG relation (Eqn. 18) for the 2DMKA and the 2DR10 models.

| Model | τ_α from | S_c type | A | α | τ_0 |
|-------|--------------------|--------------|-------|----------|------------------------|
| 2DMKA | overlap function | Harmonic | 4.33 | 0.49 | 5.55×10^{-3} |
| | $F_s(K, t)$ | Harmonic | 17.26 | 0.22 | 6.11×10^{-10} |
| | CR- $F_s(K, t)$ | Harmonic | 7.72 | 0.35 | 1.77×10^{-4} |
| | overlap function | Anharmonic 1 | 5.41 | 1.11 | 0.95 |
| | $F_s(K, t)$ | Anharmonic 1 | 6.51 | 0.97 | 0.16 |
| | CR- $F_s(K, t)$ | Anharmonic 1 | 5.86 | 0.99 | 1.14 |
| | CR- $F_s(K, t)$ | Anharmonic 2 | 5.64 | 0.95 | 1.03 |
| 2DR10 | overlap function | Harmonic | 0.65 | 2.10 | 19.12 |
| | $F_s(K, t)$ | Harmonic | 1.25 | 1.76 | 0.12 |
| | CR- $F_s(K, t)$ | Harmonic | 0.56 | 2.19 | 3.10 |
| | overlap function | Anharmonic 1 | 0.83 | 1.71 | 2.68 |
| | $F_s(K, t)$ | Anharmonic 1 | 2.11 | 1.29 | 2.89×10^{-3} |
| | CR- $F_s(K, t)$ | Anharmonic 1 | 0.72 | 1.77 | 0.49 |
| | CR- $F_s(K, t)$ | Anharmonic 2 | 0.59 | 1.96 | 4.62 |

temperature in 2D is, in fact, zero⁴⁰. In other words, there is no ideal glass transition at non-zero temperature in 2D. Given these background, the effect of the correction to S_c due to vibration entropy - see Eqns. 11, 13 - on its T dependence becomes especially interesting in 2D to which we turn our attention next.

In Fig. 6 we show the S_c data over a range of low temperatures upto the onset temperature for 2DMKA (top row) and 2DR10 (bottom row) models. First note that when the configurational entropy is computed in harmonic approximation, left columns of Fig. 6, $TS_c^{har}(T)$ is indeed linear with T . However the Kauzmann temperature T_K is significantly different from the VFT divergence temperature T_0 in both the models, see Tables I, II. We also fit the data using a non-linear function $TS_c = [K_T(\frac{T}{T_K} - 1)]^{\frac{1}{\alpha_1}}$ with α_1 as a free fit parameter. The choice of this fit function is motivated by Eqn. 18, although other fit functions have also been used in the literature³⁹. This analysis results in the exponent $\alpha_1 \sim 1$ within numerical accuracy providing a robust test of the linearity of $TS_c^{har}(T)$.

To the contrary, we find that in 2D glass-formers, adding anharmonic correction makes the TS_c^{anhar} distinctly *non-linear* with T . This behaviour is the same in both models and using both methods 1 and 2 for computing the anharmonic vibrational entropy (see Eqns. 10-13). However, estimates of T_K depends on the models and the methods of computing the anharmonic correction to S_c . On one hand, in the 2DMKA model, the non-linear fit estimate of T_K values are significantly lower when anharmonic contribution to vibrational entropy is considered, and approximately same for both methods 1 and 2. On the other hand, in the 2DR10 model, method 1 results in $T_K \sim T_0$ while method 2 produces a T_K closer to zero, see Table II. In order to gain further insight, on the right columns of Fig. 6, we show the temperature dependence of S_c . We analyze the T dependence using several plausible fitting functions which can be organized into two families: one assuming $T_K = 0^{40}$ and the other assuming $T_K \neq 0$. However, both families produce fits of comparable quality. Hence in the range of temperature in which configurational entropy is analyzed in the present study, our data is consistent with both finite and zero temperature ideal glass transition scenarios.

Finally, in Fig. 7, we test the AG relation with (main panel) and without (inset) including the anharmonic correction to the configurational entropy. Since the timescales at low temperatures gets decoupled (see Fig. 3), we consider both α -relaxation time $\tau_{\alpha CR}$ as well as diffusion coefficient D_{CR} . Note that the correction due to the effect of long wavelength fluctuations are already incorporated. Thus *Fig. 7 constitutes the main result of the present work*. The top row of Fig. 7 shows data for 2DMKA model and the bottom row depicts 2DR10 model data. Lines are fits to Eqn. 18 from which the scaling exponent α is extracted and tabulated in Table III. First, for the 2DMKA model, comparing the inset and the main panel, we see that the main effect of anharmonic correction is to reduce the deviation from the AG relation, Eqn. 1, *i.e.* to increase the value of α towards 1. This behaviour remains same for both $\tau_{\alpha CR}$ and D_{CR} . Indeed, for the 2DMKA model, the AG relation is recovered within numerical accuracy when both the correction to $\tau_{\alpha CR}$ due to long wavelength fluctuation and the correction to S_c due to anharmonic vibration are considered. Even with D_{CR} , the AG relation is only weakly non-linear for this model. To the contrary, the 2DR10 model shows a qualitatively different behaviour. Even after accounting for all the corrections in timescales and entropy, one still observes a breakdown of the AG relation in two dimensions. Thus we clearly reveal an intrinsic dimension dependence that indicates that the behavior of 2D glass-formers are different from those in 3D. Interestingly, the nature

of inter-particle interaction has a more fundamental effect in determining the value of the exponent α than long wavelength fluctuations and anharmonic correction. Although, even in 2DR10 model, including the anharmonic correction reduces the extent of deviation from linearity, *i.e.* decreases α towards 1.

V. SUMMARY AND CONCLUSION

In the present work we carefully examine whether the behaviour of glass-formers in 2D is intrinsically different from those in 3D. To this aim we test the validity of the well-known Adam-Gibbs (AG) relation between dynamics and thermodynamics in two different 2D glass-forming models. In particular, we critically examine the role of two factors that affect the dynamics and the thermodynamics respectively. First, we consider the dynamics of cage-relative, local displacement fields to eliminate the effect of Mermin-Wagner type long wavelength fluctuations that is unique to 2D. Second, we explicitly consider the anharmonic nature of vibration and implement anharmonic corrections to the configurational entropy, computed using two different methods. Recent works in literature have emphasized that even for amorphous matter in 2D, it is essential to explicitly take into account these factors before testing any theory of glass transition.

We demonstrate that even after accounting for these effects, the AG relation still breaks down in 2D, although the details crucially depends on the nature of the inter-particle interactions. This suggests that Mermin-Wagner type fluctuations does not capture all the differences in dynamics between 2D and 3D. Our analysis implies that behavior of glass-formers in 2D are intrinsically different from those in 3D. Since the two effects are independent of each other, we are able to compare the relative importance of the two factors for the validity of the AG relation. We find that the role of long wavelength fluctuations is mainly quantitative - it does not change the scaling relation between timescale and entropy qualitatively. To the contrary, the effect of anharmonicity of vibration is more significant in the temperature range we study because it can affect the AG relation in both qualitative and quantitative ways. We also verify that our data is consistent with both zero and non-zero temperature glass transition scenarios. This probably indicates that our analysis spans a temperature range that is not sufficient to resolve this issue, and one requires to sample lower temperature in equilibrium.

The question naturally arises about the origin of the observed deviation from the AG relation in 2D. Since we consider a system (2DMKA) with Lennard-Jones type interaction having an attractive component as well as a glass-former (2DR10) with purely repulsive interaction, we can systematically check a third factor - the role of inter-particle interactions. We show that the nature of deviation depends on the attractive *vs.* repulsive nature of the interaction potential. Whether a more advanced theory such as the Random First Order Transition (RFOT) theory can explain the breakdown of the AG relation in 2D is an intriguing open question. We note that the observed non-linearity of the scaling relation between timescale and entropy is consistent with RFOT theory, and our analysis implies that the RFOT scaling exponents should be material specific and not universal. However, to completely clarify this issue, one requires to compute the RFOT exponents, which we leave for a future study.

REFERENCES

- ¹Gilles Tarjus. Glass transitions may be similar in two and three dimensions, after all. *Proceedings of the National Academy of Sciences*, 114(10):2440–2442, 2017.
- ²N. D. Mermin and H. Wagner. Absence of ferromagnetism or antiferromagnetism in one- or two-dimensional isotropic heisenberg models. *Phys. Rev. Lett.*, 17:1133–1136, Nov 1966.
- ³P. C. Hohenberg. Existence of long-range order in one and two dimensions. *Phys. Rev.*, 158:383–386, Jun 1967.
- ⁴N. D. Mermin. Crystalline order in two dimensions. *Phys. Rev.*, 176:250–254, Dec 1968.
- ⁵J M Kosterlitz. Commentary on ‘ordering, metastability and phase transitions in two-dimensional systems’ j m kosterlitz and d j thouless (1973 j. phys. c: Solid state phys, 6, 1181-203) - the early basis of the successful kosterlitz-thouless theory. *Journal of Physics: Condensed Matter*, 28(48):481001, sep 2016.
- ⁶J M Kosterlitz and D J Thouless. Ordering, metastability and phase transitions in two-dimensional systems. *Journal of Physics C: Solid State Physics*, 6(7):1181–1203, apr 1973.
- ⁷David R. Nelson and B. I. Halperin. Dislocation-mediated melting in two dimensions. *Phys. Rev. B*, 19:2457–2484, Mar 1979.
- ⁸A. P. Young. Melting and the vector coulomb gas in two dimensions. *Phys. Rev. B*, 19:1855–1866, Feb 1979.

- ⁹Bernd Illing, Sebastian Fritschi, Herbert Kaiser, Christian L. Klix, Georg Maret, and Peter Keim. Mermin–wagner fluctuations in 2d amorphous solids. *Proceedings of the National Academy of Sciences*, 114(8):1856–1861, 2017.
- ¹⁰Elijah Flenner and Grzegorz Szamel. Fundamental differences between glassy dynamics in two and three dimensions. *Nature Communications*, 6(1):7392, 2015.
- ¹¹Hayato Shiba, Yasunori Yamada, Takeshi Kawasaki, and Kang Kim. Unveiling dimensionality dependence of glassy dynamics: 2d infinite fluctuation eclipses inherent structural relaxation. *Phys. Rev. Lett.*, 117:245701, Dec 2016.
- ¹²John Russo and Hajime Tanaka. Assessing the role of static length scales behind glassy dynamics in polydisperse hard disks. *Proceedings of the National Academy of Sciences*, 112(22):6920–6924, 2015.
- ¹³Skanda Vivek, Colm P. Kelleher, Paul M. Chaikin, and Eric R. Weeks. Long-wavelength fluctuations and the glass transition in two dimensions and three dimensions. *Proceedings of the National Academy of Sciences*, 114(8):1850–1855, 2017.
- ¹⁴Julian H. Gibbs and Edmund A. DiMarzio. Nature of the glass transition and the glassy state. *Journal of Chemical Physics*, 28:373–383, 1958.
- ¹⁵Gerold Adam and Julian H. Gibbs. On the temperature dependence of cooperative relaxation properties in glass-forming liquids. *The Journal of Chemical Physics*, 43(1):139–146, 1965.
- ¹⁶Pablo G. Debenedetti. *Metastable Liquids: Concepts and Principles*. Princeton University Press, 2021.
- ¹⁷TR Kirkpatrick and D Thirumalai. Colloquium: Random first order transition theory concepts in biology and physics. *Reviews of Modern Physics*, 87(1):183, 2015.
- ¹⁸Vassiliy Lubchenko and Peter G. Wolynes. Theory of structural glasses and supercooled liquids. *Annual Review of Physical Chemistry*, 58(1):235–266, 2007. PMID: 17067282.
- ¹⁹Jean-Philippe Bouchaud and Giulio Biroli. On the adam-gibbs-kirkpatrick-thirumalai-wolynes scenario for the viscosity increase in glasses. *The Journal of Chemical Physics*, 121(15):7347–7354, 2004.
- ²⁰Giulio Biroli and Jean-Philippe Bouchaud. The random first-order transition theory of glasses: a critical assessment. *Structural Glasses and Supercooled Liquids: Theory, Experiment, and Applications*, pages 31–113, 2012.
- ²¹Francis W. Starr, Jack F. Douglas, and Srikanth Sastry. The relationship of dynamical het-

- erogeneity to the adam-gibbs and random first-order transition theories of glass formation. *The Journal of Chemical Physics*, 138(12):12A541, 2013.
- ²²Smarajit Karmakar, Chandan Dasgupta, and Srikanth Sastry. Length scales in glass-forming liquids and related systems: a review. *Reports on Progress in Physics*, 79(1):016601, dec 2015.
- ²³Shiladitya Sengupta, Smarajit Karmakar, Chandan Dasgupta, and Srikanth Sastry. Adam-gibbs relation for glass-forming liquids in two, three, and four dimensions. *Phys. Rev. Lett.*, 109:095705, Aug 2012.
- ²⁴Francesco Sciortino. Potential energy landscape description of supercooled liquids and glasses. *Journal of Statistical Mechanics: Theory and Experiment*, 2005(05):P05015, may 2005.
- ²⁵Ujjwal Kumar Nandi, Palak Patel, Mohd Moid, Manoj Kumar Nandi, Shiladitya Sengupta, Smarajit Karmakar, Prabal K. Maiti, Chandan Dasgupta, and Sarika Maitra Bhattacharyya. Thermodynamics and its correlation with dynamics in a mean-field model and pinned systems: A comparative study using two different methods of entropy calculation. *The Journal of Chemical Physics*, 156(1):014503, 2022.
- ²⁶Pallabi Das and Srikanth Sastry. Crossover in dynamics in the kob-andersen binary mixture glass-forming liquid. *Journal of Non-Crystalline Solids: X*, 14:100098, 2022.
- ²⁷Shiladitya Sengupta, Filipe Vasconcelos, Frédéric Affouard, and Srikanth Sastry. Dependence of the fragility of a glass former on the softness of interparticle interactions. *The Journal of Chemical Physics*, 135(19):194503, 2011.
- ²⁸D. Brown and J.H.R. Clarke. A comparison of constant energy, constant temperature and constant pressure ensembles in molecular dynamics simulations of atomic liquids. *Molecular Physics*, 51(5):1243–1252, 1984.
- ²⁹Walter Kob and Hans C. Andersen. Testing mode-coupling theory for a supercooled binary lennard-jones mixture i: The van hove correlation function. *Phys. Rev. E*, 51:4626–4641, May 1995.
- ³⁰Ralf Brüning, Denis A St-Onge, Steve Patterson, and Walter Kob. Glass transitions in one-, two-, three-, and four-dimensional binary lennard-jones systems. *Journal of Physics: Condensed Matter*, 21(3):035117, dec 2008.
- ³¹Smarajit Karmakar, Anael Lemaître, Edan Lerner, and Itamar Procaccia. Predicting plastic flow events in athermal shear-strained amorphous solids. *Phys. Rev. Lett.*, 104:215502,

May 2010.

- ³²Kurt Binder and Walter Kob. *Glassy Materials and Disordered Solids*. WORLD SCIENTIFIC, revised edition, 2011.
- ³³Anshul D. S. Parmar, Shiladitya Sengupta, and Srikanth Sastry. Length-scale dependence of the stokes-einstein and adam-gibbs relations in model glass formers. *Phys. Rev. Lett.*, 119:056001, Jul 2017.
- ³⁴T. R. Kirkpatrick, D. Thirumalai, and P. G. Wolynes. Scaling concepts for the dynamics of viscous liquids near an ideal glassy state. *Phys. Rev. A*, 40:1045–1054, Jul 1989.
- ³⁵Srikanth Sastry. The relationship between fragility, configurational entropy and the potential energy landscape of glass-forming liquids. *Nature*, 409:164–167, 2001.
- ³⁶Vladimir N. Novikov and Alexei P. Sokolov. Temperature dependence of structural relaxation in glass-forming liquids and polymers. *Entropy*, 24(8), 2022.
- ³⁷R. Richert and C. A. Angell. Dynamics of glass-forming liquids. v. on the link between molecular dynamics and configurational entropy. *The Journal of Chemical Physics*, 108(21):9016–9026, 1998.
- ³⁸Atreyee Banerjee, Manoj Kumar Nandi, Srikanth Sastry, and Sarika Maitra Bhattacharyya. Effect of total and pair configurational entropy in determining dynamics of supercooled liquids over a range of densities. *The Journal of Chemical Physics*, 145(3):034502, 2016.
- ³⁹Misaki Ozawa, Camille Scalliet, Andrea Ninarello, and Ludovic Berthier. Does the adam-gibbs relation hold in simulated supercooled liquids? *The Journal of Chemical Physics*, 151(8):084504, 2019.
- ⁴⁰Ludovic Berthier, Patrick Charbonneau, Andrea Ninarello, Misaki Ozawa, and Sho Yaida. Zero-temperature glass transition in two dimensions. *Nature Communications*, 10(1508), 2019.